1-1-2017

Freedericksz Transition in Nematic Liquid Crystal Couette Flow

Arup Mukherjee
Montclair State University, mukherjeea@mail.montclair.edu

Advances and Applications in Fluid Mechanics
http://www.pphmj.com
http://dx.doi.org/10.17654/FM020010169
Volume 20, Number 1, 2017, Pages 169-183 **ISSN: 0973-4686**

FREEDERICKSZ TRANSITION IN NEMATIC LIQUID CRYSTAL COUETTE FLOW

Arup Mukherjee

Department of Mathematical Sciences
Montclair State University
Montclair, NJ 07043, U. S. A.

Abstract

This article investigates the effects of an external magnetic field on the Freedericksz transition for an elastically anisotropic nematic liquid crystal sample occupying the annular region between two concentric cylinders in relative (slow) rotation. Assuming both azimuthal and radial magnetic fields and strong anchoring conditions for the liquid crystal director perpendicular to the surface of the cylinders, we investigate and characterize the differences in the director distortions and the critical field value for the onset of the transition.

1. Introduction

The molecular re-orientation of nematic liquid crystals (NLCs) under the action of applied external fields is called a *Freedericksz transition*. This re-orientation phenomenon is useful in the control of many liquid Crystal (LC) devices and as an experimental technique for determining the elastic constants of an LC [1, 2]. The preferred direction in any liquid crystal is

Received: October 26, 2016; Accepted: December 17, 2016
2010 Mathematics Subject Classification: 76A15, 82D30.
Keywords and phrases: Freedericksz transition, Couette flow, elastic anisotropy.
Communicated by Shahrdad G. Sajjadi

represented by a smoothly varying unit vector **n** called the *director*. Due to intermolecular interactions, the elongated rod-like molecules of nematic liquid crystals orient themselves parallel to **n**. For a static NLC sample under the effect of an external magnetic field, the equilibrium director alignment is determined by a balance between the forces generated by the applied field and the surface boundary effects (anchoring effects). Low field intensities are unable to overcome the re-orientation threshold for the elastic energy of the NLC, resulting in a uniform director orientation determined by the anchoring. On the other hand, for field intensities beyond a critical value, the NLC undergoes a Freedericksz transition and the equilibrium state for **n** is non-uniform. Derfel [3] used methods from catastrophe theory to re-analyze previously known Freedericksz transition effects in a static NLC to re-state the phenomenon as a bifurcation problem. Blake et al. [4] extended this work to analyze the effects of imperfections in the anchoring at the boundaries. Considering an NLC between two parallel plates, the combined influence of an external magnetic field and a linear shear flow was studied by Mukherjee and Mukherjee [5, 7] and Makarov and Zakhlevnykh [6].

Atkin and Leslie [8] analyzed the solution and scaling analysis for Couette flow of NLCs in the absence of magnetic fields, while Currie [9] extended the study by deriving the governing equations for helical flow of NLC in the presence of a magnetic field and characterizing the possible solutions. Kini [10] discussed how the shear rate and magnetic field strength affects the apparent viscosity of an NLC. In this paper, we consider the steady state Couette flow of an NLC occupying the annular region between two concentric cylinders in relative rotation and subject to an applied external magnetic field having both radial and azimuthal components. By following the methodology of Makarov and Zakhlevnykh [6] and Mukherjee and Mukherjee [5, 7], we analyze the combined effect of flow, field, and elastic anisotropy on flow patterns and the critical value of the transition. Our numerical study shows that the sharp Freedericksz transition present in a static nematic is smoothed out due to a shear component in the flow introduced as an effect of relative rotation of the cylinders. We find that the onset of transition is directly related to the apparent viscosity of the

NLC which decreases with increasing azimuthal field strength. We further demonstrate that for fields with a non-zero radial component, a non-uniform equilibrium state of the director exists for all non-zero magnetic field strengths.

In Section 2, we summarize the Frank-Oseen elastic energy governing static NLC behavior, and the nematodynamic equations of Ericksen and Leslie. In Section 3, we introduce the geometry we study, and derive the boundary value problem for the director **n** under simplifying assumption. Finally, Section 4 discusses our findings, and Section 5 provides a summary.

2. Elastic Energy and Nematodynamic Equations

For incompressible NLCs, the unit vector field $\mathbf{n}(\mathbf{x})$ represents the mean molecular alignment of a point **x** in a given sample of volume V with boundary S. Positivity of the free energy density $\mathcal{F}$, symmetry properties arising from lack of polarity, and the rod-like nature of NLC molecules which are indistinguishable under reflection within planes containing the director **n**, leads to the Frank-Oseen elastic energy density given by

$$\mathcal{F}_{\text{el}}(\mathbf{n}, \nabla\mathbf{n}) = \frac{1}{2}K_1|\nabla\cdot\mathbf{n}|^2 + \frac{1}{2}K_2|\mathbf{n}\cdot(\nabla\times\mathbf{n})|^2 + \frac{1}{2}K_3|\mathbf{n}\times(\nabla\times\mathbf{n})|^2, \quad (1)$$

where the constants K_1, K_2 and K_3 correspond to the splay, twist, and bend elasticity (or Frank) constants. For any energy density of the form $\mathcal{F}(\mathbf{n}, \nabla\mathbf{n})$ given in (1), the total elastic energy is given by $W = \int_V \mathcal{F}(\mathbf{n}, \nabla\mathbf{n})dV$. For nematic liquid crystal's the *elastic anisotropy* $k = K_3/K_1$ satisfies $k \geq 1$. External magnetic fields applied to an NLC encourages the director to align parallel to the field in the bulk of the sample. A magnetic field **H** applied to an LC sample induces a magnetization **M** in the sample. If $\chi_{||}$ and $\chi_{\perp}$ represent the magnetic susceptibilities along and perpendicular to **n**, and we assume a linear relationship between **M** and the applied field **H**, the invariance of the elastic energy density under the transformation $\mathbf{n} \mapsto -\mathbf{n}$ leads to the expression $\mathbf{M} = \chi_{\perp}\mathbf{H} + (\chi_{||} - \chi_{\perp})(\mathbf{H}\cdot\mathbf{n})\mathbf{n} = \chi_{\perp}\mathbf{H} + \chi_a(\mathbf{H}\cdot\mathbf{n})\mathbf{n}$, where $\mathbf{H}$ makes an arbitrary angle with $\mathbf{n}$ and the magnetic anisotropy χ_a measures the difference between the magnetic susceptibilities. For NLCs, $\chi_a > 0$. Thus, when an external magnetic field $\mathbf{H}$ is applied to a static NLC, the elastic energy of equation (1) is modified by the magnetic energy density $\mathcal{F}_{\text{mg}} = \int_0^H \mathbf{M} \cdot d\mathbf{H}$ to yield the energy density

$$\mathcal{F} = \mathcal{F}_{\text{el}} - \mathcal{F}_{\text{mg}} = \mathcal{F}_{\text{el}} - \frac{1}{2}\chi_{\perp}H^2 - \frac{1}{2}\chi_a(\mathbf{n} \cdot \mathbf{H})^2, \text{ where } H = |\mathbf{H}|. \quad (2)$$

The alignment of the director at the boundary surfaces within which the liquid crystal sample is contained is called *anchoring*. Strong anchoring describes a scenario where the surface forces at the rigid boundaries are large enough to impose a clearly defined direction for $\mathbf{n}$ at the boundary. When the NLC sample aligns parallel to the boundary the anchoring is planar, while homeotropic anchoring corresponds to a perpendicular alignment. In this article, we assume that the NLC is homeotropically anchored at the two bounding cylinders containing the sample.

A standard description of the motion of a fluid with microstructure involves the velocity, $\mathbf{v}(\mathbf{x}, t)$, and angular velocity $\mathbf{w}(\mathbf{x}, t)$ fields. For LCs, $\mathbf{w}$ represents the local angular velocity of the director $\mathbf{n}$. Thus, the unit vector $\mathbf{n}$ satisfies $\dot{\mathbf{n}} = \mathbf{w} \times \mathbf{n}$, where $\dot{\mathbf{n}} = \frac{\partial \mathbf{n}}{\partial t} + \mathbf{v} \cdot \frac{\partial \mathbf{n}}{\partial \mathbf{x}}$ is the material time derivative. If $p = p(\mathbf{x}, t)$ is the pressure, ρ is the density, and $\mathbf{F}$ and $\mathbf{G}$ are the external and generalized body forces, the Ericksen-Leslie nematodynamic equations for an incompressible LC sample occupying a region $V \subseteq \mathbb{R}^3$ with boundary S are

$$n_i n_i = 1 \text{ and } v_{i,i} = 0, \quad (3)$$

$$\rho\dot{v}_i = \rho F_i - (p + \mathcal{F})_{,i} + \tilde{g}_j n_{j,i} + G_j n_{j,i} + \tilde{t}_{ij,j} \text{ and} \quad (4)$$

$$\left(\frac{\partial \mathcal{F}}{\partial n_{i,j}}\right)_{,j} - \frac{\partial \mathcal{F}}{\partial n_i} + \tilde{g}_i + G_i = \lambda n_i, \quad (5)$$

where λ is a Lagrange multiplier and can be eliminated. The constitutive equations (arising from the material properties of the LC) for the viscous stress $\tilde{t}_{ij}$ and the vector $\tilde{g}_i$ are determined using the rate of strain tensor $A_{ij} = \frac{1}{2}(v_{i,j} + v_{j,i})$, the vorticity tensor $W_{ij} = \frac{1}{2}(v_{i,j} - v_{j,i})$, the rate of change of the director relative to the background fluid $N_i = \dot{n}_i - W_{ij}n_j$, and the Leslie coefficients $\alpha_i, 1 \leq i \leq 6$ as

$$\tilde{t}_{ij} = \alpha_1 n_k A_{kp} n_p n_i n_j + \alpha_2 N_i n_j + \alpha_3 n_i N_j + \alpha_4 A_{ij} + \alpha_5 n_j A_{ik} n_k + \alpha_6 n_i A_{jk} n_k, \tag{6}$$

and

$$\tilde{g}_i = -\gamma_1 N_i - \gamma_2 A_{ip} N_p, \tag{7}$$

where $\gamma_1 = \alpha_3 - \alpha_2 \geq 0$ and $\gamma_2 = \alpha_3 + \alpha_2$ are the rotational viscosity and torsion coefficient, and the Parodi's relation $\alpha_2 + \alpha_3 = \alpha_6 - \alpha_5$ holds. Due to the constraint imposed by Parodi's relation, only five of the Leslie coefficients are independent and are assumed to form a canonical set of viscosities for the LC. For this nematodynamic model, the Cauchy stress tensor is related to the pressure, elastic energy, and the viscous stress via $t_{ij} = -p\delta_{ij} - \frac{\partial \mathcal{F}}{\partial n_{p,j}} n_{p,i} + \tilde{t}_{ij}$.

3. Couette Flow and Freedericksz Transition

In this paper, we consider a sample of NLC occupying the annular region between two concentric cylinders with radii R_1 and R_2 in relative rotation as shown in Figure 1 and seek steady state solutions for the velocity **v** and director **n** under the effect of external magnetic fields. Assuming that flow properties are determined by the combined effect of the coaxial cylinders rotating with angular velocities Ω_1 and Ω_2 and an external magnetic field **H** with no component along the cylinder axis, we consider the following forms for the velocity, director, and magnetic field in cylindrical polar coordinates:

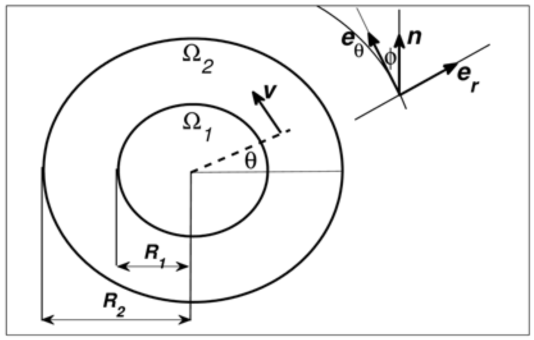

Figure 1. The set up for Couette flow in $R_1 \le r \le R_2$ with the outer (resp. inner) cylinder having angular velocity Ω_1 (resp. Ω_2). The z-axis of the usual cylindrical polar coordinate system (r, θ, z) is perpendicular to the page. The director $\mathbf{n}$ makes an angle ϕ with the unit vector $\mathbf{e}_\theta$. The velocity $\mathbf{v}$ is parallel to $\mathbf{e}_\theta$.

$$\mathbf{H} = (H_r, H_\theta, 0) = (A/r, B/r, 0), \tag{8}$$

$$\mathbf{v} = (0, v_\theta, 0) = (0, r\omega(r), 0), \tag{9}$$

and

$$\mathbf{n} = (\sin\phi(r), \cos\phi(r), 0). \tag{10}$$

The constraints (3) are automatically satisfied by the forms (9) and (10). Usual no-slip boundary conditions for the velocity and the fact that $\mathbf{n}$ and $-\mathbf{n}$ are equivalent result in

$$\omega(R_i) = \Omega_i \text{ and } \phi(R_i) = \pm\pi/2 \text{ for } i = 1, 2 \tag{11}$$

as the boundary conditions on $\omega(r)$ and $\phi(r)$. We observe that when $A = 0$ and $B \ne 0$, the aligning effect of the azimuthal magnetic field and the homeotropic anchoring act against one another. When the magnitude of B is small, the director **n** remains undistorted and the transition occurs beyond a critical value of B. However, when $A,\ B \neq 0,$ even small intensities of the applied field yield distorted equilibrium states for **n**.

Using the expressions for **v** and **n** in the linear and angular momentum equations (4) and (5), and eliminating $\frac{d\omega}{dr}$ yields

$$f(\phi)r^2\left[\frac{d^2\phi}{dr^2} + \frac{1}{r}\frac{d\phi}{dr}\right] + \frac{1}{2}r^2\frac{df(\phi)}{d\phi}\left[\frac{1}{r^2} + \left(\frac{d\phi}{dr}\right)^2\right]$$

$$= -\frac{\chi_a}{2K_1}[(A^2 - B^2)\sin 2\phi + AB\cos 2\phi] + \frac{c\gamma_1}{2K_1 g(\phi)}(1 - \gamma\cos 2\phi), \quad (12)$$

where $f(\phi) = \cos^2\phi + k\sin^2\phi,$ c is a measure of the magnitude of the moment per unit length on either cylinder, and $g(\phi) = \frac{1}{2}[2\alpha_1\sin^2\phi\cos^2\phi +$ $(\alpha_5 - \alpha_2)\sin^2\phi + (\alpha_3 + \alpha_6)\cos^2\phi + \alpha_4].$ The function $f(\phi) \equiv 1$ and the term involving the derivative of $f(\phi)$ is absent when $k = 1.$ Moreover, the function $g(\phi)$ always satisfies $g(\phi) \geq 0,$ and equals the Newtonian viscosity $\frac{1}{2}\alpha_4$ for isotropic fluids. For our analysis in this article, we will assume $g(\phi) > 0.$ When $c = 0,$ the velocity $\omega(r)$ is a constant so that the motion corresponds to a uniform rigid body motion. Note that $c > 0$ (respectively, < 0) if $\Omega_2 > \Omega_1$ (respectively, $\Omega_2 < \Omega_1$) corresponds to the outer (respectively, inner) cylinder rotating faster. The parameter $\gamma = -\gamma_2/\gamma_1$ is the reactive parameter. When $\gamma \geq 1,$ the flow alignment angle is defined as $\cos 2\phi_L = 1/\gamma$ [2]. If we consider the sample to be an anisotropic fluid, then $\phi(r) \equiv \phi_L.$

Re-scaling the independent variable $R_1 \leq r \leq R_2$ to $0 \leq \tilde{r} \leq 1$ using $\tilde{r}(R_2 - R_1) = r - R_1$ and re-writing equation (12) when the magnetic field is purely azimuthal $(A = 0),$ we get

$$f(\phi)(\tilde{r}R + R_1)^2\left[\frac{d^2\phi}{d\tilde{r}^2} + \frac{R}{\tilde{r}R + R_1}\frac{d\phi}{d\tilde{r}}\right]$$

$$+\frac{1}{2}(\tilde{r}R + R_1)^2\frac{df(\phi)}{d\phi}\left[\frac{R^2}{(\tilde{r}R + R_1)^2} + \left(\frac{d\phi}{d\tilde{r}}\right)^2\right]$$

$$= +\frac{\chi_a R^2 B^2}{2K_1}\sin 2\phi + \frac{c\gamma_1 R^2}{2K_1}\frac{1}{g(\phi)}(1 - \gamma\cos 2\phi), \tag{13}$$

where $R = R_2 - R_1$ is the gap width between the cylinders and $\phi = \phi(\tilde{r})$ satisfies the boundary conditions $\phi(0) = \phi(1) = \pm\pi/2$. The parameter $\lambda \doteq \chi_a R^2 B^2/2K_1$ is proportional to the square of the magnetic field strength, while $\mu \doteq c\gamma_1 R^2/2K_1$ is proportional to the magnitude of the moment per unit length on the cylinders. The relative angular velocity and the apparent viscosity are determined by the relations

$$\Delta\Omega = \Omega_2 - \Omega_1 = c\int_{R_1}^{R_2}\frac{1}{r^3 g(\phi)}dr \text{ and } \eta = \frac{c(R_2^2 - R_1^2)}{2(R_1R_2)^2\Delta\Omega}, \tag{14}$$

and can be computed once ϕ is determined. For low shear rates η remains almost constant at the value $\eta_2 = \frac{1}{2}(-\alpha_2 + \alpha_4 + \alpha_5)$ until B reaches a critical value B_c. When $B > B_c$ there is a rapid change of η with field strength and for large B, η quickly approaches the value $\eta_1 = \frac{1}{2}(\alpha_3 + \alpha_4 + \alpha_6)$. If $K_3 = K_1 = K$, the critical value of the azimuthal field satisfies the relation $B_c^2 = \pi R_1 K/R^2\chi_a$ (equivalently, $\lambda_c = \frac{1}{2}(R_1\pi)^2$) which corresponds to the Freedericksz threshold for a static NLC. For a detailed discussion and study of the effects of both azimuthal and radial fields on the apparent viscosity, see Kini [10]. For any shear rate, the extremum of ϕ occurs at a point $r_m = (R_1R_2)^{1/2}$ (see, for example [2, pp. 206-209]). When

$\frac{1}{2}(R_1 + R_2) \gg R,\ r_m \approx \frac{1}{2}(R_1 + R_2)$ and the orientation profile is almost symmetric. Since we always assume $R_1 = 1,\ R_2 = 1.001$ for this article, the orientation profiles for the director are expected to be symmetric. The boundary value problem (13) is very similar to the boundary value problem for determining the director angle for an NLC between two parallel plates subject to a shear and an external magnetic field perpendicular to the plates. For a detailed discussion of the combined effects of shear, elastic anisotropy, and external field in this case, see Mukherjee and Mukherjee [7] and the references cited there.

4. Results and Discussion

We now study the combined effect of the magnetic field strength, elastic anisotropy, and shear rate on the flow pattern and the Freedericksz threshold. In particular, we solve the boundary value problem (13) and study the bifurcation patterns. The boundary value problems are solved using the software XPPAUT [11] which can track solutions through turning points and branch points. Since the elastic anisotropy coefficient k and the reactive parameter γ are ratios of similar NLC coefficients, they are unit independent. We assume $R_1 = 1$ and a gap width of $R = 10^{-3}$, so that the critical value of the static Freedericksz transition is $B_c = \pi^2/2 \approx 4.93$. All figures in Section 4 represent the maximum director distortion $\phi_m = \phi(\tilde{r}_m)$ as a function of the magnetic field strength parameter λ. The specific values of the NLC materials used for our study are given in Table 1. The values for 5CBI are taken from [12, 13, 14] where the special choices $\alpha_1 = 0$ and $k = 1$ in 5CBI are justified, while the values for MBBA at 25° and PAA at 122° are from [2, pp. 330]. While the coefficients for MBBA and PAA are based on actual experimental data, 5CBI is an idealized version of the NLC 5CB.

Table 1. Physical parameters for 5CBI, MBBA near 25° and PAA near 122°

Quantity	5CBI	MBBA	PAA
α_1	0	-0.0181	0.0043
α_2	-0.04815	-0.1104	-0.0069
α_3	-0.00315	-0.001104	-0.0002
α_4	0.0512	0.0826	0.0068
α_5	0.03765	0.0779	0.0047
α_6	-0.01365	-0.0336	-0.0023
K_1	0.4×10^{-11}	0.6×10^{-11}	0.69×10^{-11}
K_2	0.4×10^{-11}	0.38×10^{-11}	0.38×10^{-11}
K_3	0.4×10^{-11}	0.75×10^{-11}	1.19×10^{-11}
γ, k	1.14, 1	$1.\overline{02}$, 1.25	1.014, 1.72

4.1. Shear effects (MBBA)

Figure 2 shows the variation of the maximum director distortion ϕ_m as a function of the magnetic field strength parameter λ for MBBA. All three curves in the figure correspond to the inner cylinder rotating faster than the outer one $(\mu < 0 \text{ or } \Omega_1 > \Omega_2)$. When the shear rate is very small, the director is uniform for small field intensities while it undergoes a sharp transition once the azimuthal magnetic field crosses a threshold value. The threshold for this Freedericksz transition like effect is higher than the static threshold value of $\lambda_c \approx 4.93$. For small λ, $\eta \approx \eta_2$ the larger of the two viscosities determined by the Leslie coefficients. Thus, for small values of λ, the undisturbed director state corresponding to an NLC without the magnetic field persists. However, when η crosses the threshold, the effective viscosity η quickly decreases to the lower viscosity η_1 and this allows for director re-orientation. Since the effective viscosity of the NLC does not decrease below η_1, $\phi_m \to \phi_L$ for large values of λ. For MBBA, the flow alignment angle $\phi_L \approx -0.1$, and we see this asymptotic behavior in Figure 2. For larger values of the shear rate, the sharp nature of the transition is smoothed out. For example, when $\mu = -0.1$, the NLC molecules are at an equilibrium state corresponding to $\phi_m > -\pi/2$ even when $\lambda = 0$. This smoothing behavior is similar to the smoothing of the Freedericksz transition observed when a shear flow is imposed on an NLC sample between parallel plates and under the influence of an external magnetic field perpendicular to the plates [6].

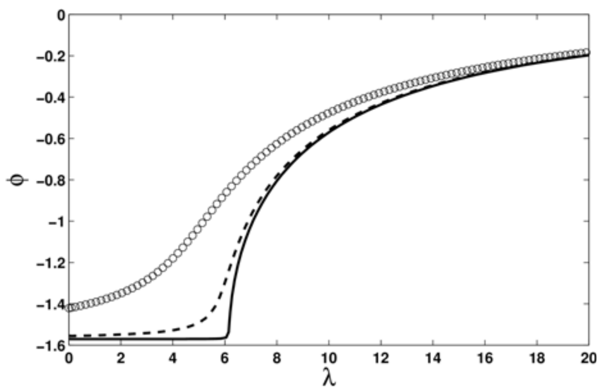

Figure 2. Maximum angle ϕ_m and λ for MBBA with azimuthal $(A = 0)$ field. Slow shear rate (line, $\mu = -0.0001$), medium shear rate (dashed, $\mu = -0.01$), and high shear rate (circle, $\mu = -0.1$).

4.2. Elastic anisotropy effects (MBBA)

Figure 3 shows the effect of elastic anisotropy on the onset of Freedericksz transition for MBBA. We observe that when the shear rate is very small, the threshold value of the transition can be very close to the static limit $\lambda_c \approx 4.93$ if elastic isotropy is imposed on the NLC. The behavior of an elastically anisotropic sample of MBBA is similar to the artificially isotropic sample. However, for the elastically anisotropic sample, the threshold for the onset of transition is higher. As the applied azimuthal magnetic field increases, the difference in the values of ϕ_m for the elastically isotropic and anisotropic material decreases. This is a result of the strength of the magnetic field driving the apparent viscosity to the limiting value η_1 in both cases. For higher shear rates (not shown), we observe a similar phenomenon. The artificially elastically isotropic sample always has a higher value of ϕ_m corresponding to any field strength, but the difference goes to zero with increasing λ.

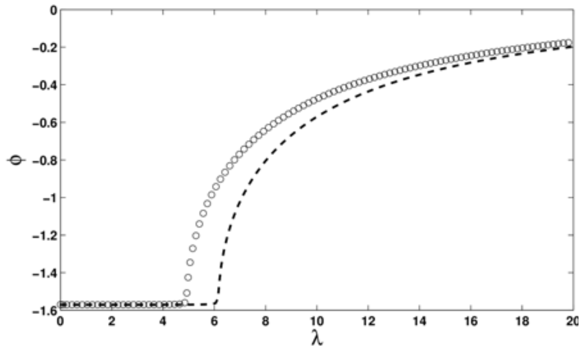

Figure 3. Maximum angle ϕ_m and λ for MBBA with azimuthal $(A = 0)$ field. Elastically Anisotropic (dashed, $k = K_3/K_1 = 1.25$), and Isotropic (circle, $k = 1$). Low shear rate $(\mu = -0.0001)$.

4.3. Non-azimuthal field effects (MBBA)

Figure 4 compares the effect of imposing purely azimuthal and mixed azimuthal and radial external fields for MBBA under a shear $\mu = 0.01$ corresponding to the outer cylinder rotating faster than the inner one. When the applied field is purely azimuthal, the magnetic field strength parameter $\lambda \propto B^2$, while $\lambda \propto AB$ when radial and azimuthal fields of equal magnitude are imposed. From equation (12), we notice that for $c = 0$ and $A = 0$, the uniform solution $\phi(r) = \pi/2$ solves the boundary value problem with boundary conditions $\phi(R_i) = \pi/2$ for all values of λ. When the applied azimuthal field is strong enough, a non-uniform director orientation is energetically preferred by the NLC. The maximum director distortion of this non-uniform equilibrium state is ϕ_m. A smoothed out version of this transition phenomenon persists when $c \neq 0$ as long as the applied field is purely azimuthal. Since the shear rate considered in Figure 4 is reasonably large, this transition threshold is not clearly defined (dashed line). However, when $A = B$ or $A = B/4$, inspection of equation (12) reveals that the uniform solution $\phi(r) = \pi/2$ does not solve the differential equation for any non-zero λ even when $c = 0$. Thus, it is not surprising that in these two cases (solid line and circle), the maximum director distortion ϕ_m deviates from the uniform solution determined by the boundary conditions $\phi(R_i) = \pi/2$ for all $\lambda \neq 0$ in Figure 4. When a component of the radial field is present, the magnitude of the limiting value of ϕ_m will be smaller than for a purely azimuthal field. As we observe in Figure 4, the limiting value of ϕ_m decreases with an increase in the proportion of the radial field component A in λ.

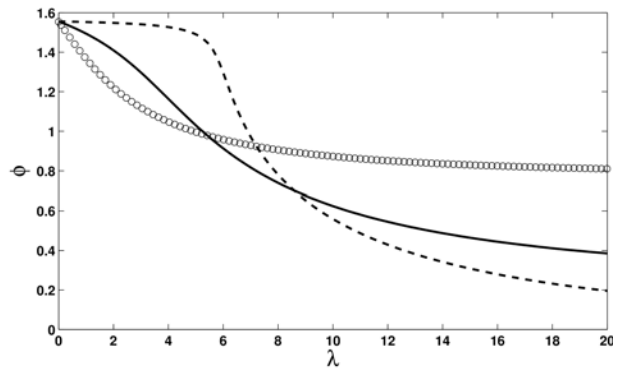

Figure 4. Maximum (in magnitude) angle ϕ_m and λ for MBBA. Azimuthal $A = 0$, $B \neq 0$, $\lambda \propto B^2$ field (dashed), equal strength radial and azimuthal field $A = B$, $\lambda \propto AB$ (circle), and weaker radial field $A = B/4$, $\lambda \propto AB/4$ (line). Medium strength shear $(\mu = 0.01)$.

4.4. Various NLC (5CBI, MBBA, PAA)

Figure 5 shows the maximum director deviation for MBBA, PAA, and 5CBI subject to an azimuthal magnetic field and a negative shear which corresponds to the inner cylinder rotating faster than the outer one. For small values of λ, elastic anisotropy determines the nature of the solutions. The NLC with the highest elastic anisotropy (PAA) shows the maximum deviation from the uniform director orientation determined by the boundary anchoring $\phi(R_i) = -\pi/2$, while the behavior of elastically isotropic NLC 5CBI is very close to the sharp transition for static NLCs.

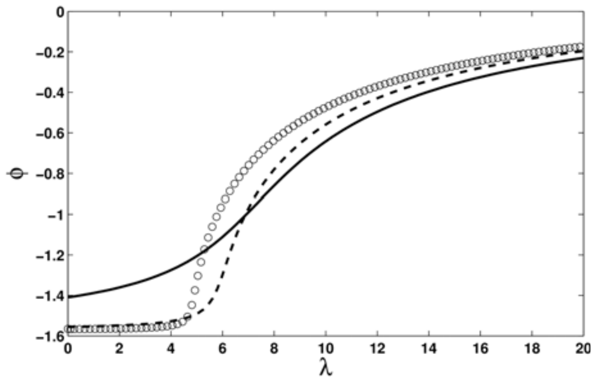

Figure 5. Maximum angle ϕ_m and λ for NLC with azimuthal $(A = 0)$ field. MBBA (dashed), PAA (line), and 5CBI (circle). Medium strength shear $(\mu = -0.01)$.

5. Summary

We have analyzed the combined effects of an external magnetic field and elastic anisotropy on an NLC occupying the annular region between two concentric cylinders in relative rotation. We show that for MBBA, the sharp Freedericksz transition of a static nematic is smoothed out when the relative rotation of the cylinders introduces a shear component to the flow. The transition is directly related to the apparent viscosity of the NLC which decreases with increasing azimuthal field strength. For high enough values of the shear, non-uniform equilibrium states are possible even in the absence of an external field. Further, the elastic isotropy assumption reduces the critical field strength at which the onset of transition occurs. However, for large enough purely azimuthal fields, the maximum director distortion always approaches a limiting value determined by the flow alignment angle ϕ_L. The magnitude of ϕ_L is determined by the reactive parameter γ. When the applied external field has a non-zero radial component, a non-uniform equilibrium state of the director exists for all non-zero magnetic field strengths and the limiting value of ϕ_m for large λ diminishes with increasing contribution of the radial component of the applied field. The qualitative behavior for different flow-aligning NLCs is the same.

References

[1] S. Chandrasekhar, Liquid Crystals, Cambridge University Press, 1992.

[2] I. W. Stewart, The Static and Dynamic Continuum Theory of Liquid Crystals, Taylor & Francis, 2004.

[3] G. Derfel, Liq. Cryst. 3 (1988), 1411.

[4] G. I. Blake, T. Mullin and S. J. Tavener, Dyn. Stab. Syst. 14 (1999), 299.

[5] A. Mukherjee and B. Mukherjee, Phys. Rev. E 71 (2005), 021703.

[6] D. V. Makarov and A. N. Zakhlevnykh, Phys. Rev. E 74 (2006), 041710.

[7] B. Mukherjee and A. Mukherjee, Mol. Cryst. Liq. Cryst. (submitted).

[8] R. J. Atkin and F. M. Leslie, Q. J. Mech. Appl. Math. 23 (1970), 53.

[9] P. K. Currie, Arch. Ration. Mech. Anal. 87(22) (1970), 222.

[10] U. D. Kini, Pramana 7(4) (1976), 223.

[11] B. Ermentrout, Simulating, Analyzing, and Animating Dynamical Systems, SIAM, 2002.

[12] H. Kneppe, F. Schneider and N. K. Sharma, Ber. Bunsenges. Phys. Chem. 85 (1981), 784.

[13] H. Kneppe, F. Schneider and N. K. Sharma, J. Chem. Phys. 77 (1982), 3203.

[14] F. M. Leslie, J. G. McIntosh and D. M. Sloan, Contin. Mech. Thermodyn. 9 (1997), 293.